

## Article

# Characterization of Different Types of Crystallization from Cocoa Butter by Using Terahertz Spectroscopy

Chao-Hui Feng <sup>1,2,\*</sup> , Chiko Otani <sup>2,3</sup> and Hiromichi Hoshina <sup>2,\*</sup> 

<sup>1</sup> School of Regional Innovation and Social Design Engineering, Faculty of Engineering, Kitami Institute of Technology, 165 Koen-cho, Kitami 090-8507, Hokkaido, Japan

<sup>2</sup> RIKEN Centre for Advanced Photonics, RIKEN, 519-1399 Aramaki-Aoba, Aoba-ku, Sendai 980-0845, Miyagi, Japan; otani@riken.jp

<sup>3</sup> Department of Physics, Tohoku University, 6-3 Aramaki-Aoba, Aoba-ku, Sendai 980-0845, Miyagi, Japan

\* Correspondence: feng.chaohui@mail.kitami-it.ac.jp (C.-H.F.); hoshina@riken.jp (H.H.)

**Abstract:** Three different cocoa butter polymorphs have been determined by X-ray diffraction (XRD) and terahertz spectroscopy in the range of 0–11 THz. Specific procedures to produce different types of crystallization were detailed. The results from XRD analysis showed that the three polymorphic forms of cocoa butter were  $\alpha$ ,  $\beta'$  (III), and  $\beta$  (V) forms. Terahertz spectroscopy showed different features according to different types of crystallization forms. An observable sharp peak at 6.80 THz can be detected from  $\beta$  (V) type and original samples, whilst  $\alpha$  type presented the broad peak at this frequency, respectively. Peaks at 4.25 THz and 5.21 THz were detected in  $\beta$  type (V) form, whilst no noticeable peaks were observed from other samples at those frequencies. This study innovatively showed a great potential to apply terahertz spectroscopy to control the tempering during chocolate manufacturing.

**Keywords:** cocoa butter; crystallization; terahertz spectroscopy; X-ray diffraction; noninvasive detection



**Citation:** Feng, C.-H.; Otani, C.; Hoshina, H. Characterization of Different Types of Crystallization from Cocoa Butter by Using Terahertz Spectroscopy. *Appl. Sci.* **2024**, *14*, 35. <https://doi.org/10.3390/app14010035>

Academic Editors: Matt Oehlschlaeger and Mona M. Hella

Received: 26 November 2023

Revised: 13 December 2023

Accepted: 15 December 2023

Published: 20 December 2023



**Copyright:** © 2023 by the authors. Licensee MDPI, Basel, Switzerland. This article is an open access article distributed under the terms and conditions of the Creative Commons Attribution (CC BY) license (<https://creativecommons.org/licenses/by/4.0/>).

## 1. Introduction

Chocolate is one of the most-craved food products in the world [1,2], with approximately 7.3 million tons consumed at retail chocolate confectioneries throughout the world in 2015/2016 and up to 7.7 million tons by 2018/2019 [2]. Cocoa butter, as a vital ingredient of chocolate, attributed to the gloss, texture, and typical melting behavior of chocolate. Due to its remarkably narrow melting range between 32 and 35 °C (equivalent to body temperature), it transfers in a very quick meltdown in the mouth, leading to a cool sensation and good flavor release [3]. The main fatty acids (FA) of cocoa butter are palmitic (P, C16:0), stearic (St, C18: 0), and oleic (O, C18:1) acid, which accounts, on average, for 26%, 36%, and 34% of the total FA composition, respectively. This simple fatty acid composition leads to a comparable simple triacylglycerol (TAG) distribution, which mainly comprises 1,3-dipalmitoyl-2-oleoyl-glycerol (POP), rac-palmitoyl-stearoyl-2-oleoyl-glycerol (POST), and 1,3-stearoyl-2-oleoyl-glycerol (StOSt) [4]. Cocoa butters differ by country of origin, leading to the different saturated stages of TAG composition. For instance, the cocoa butter from Brazil is classified as soft butter, while butter from Malaysia is regarded as hard butter, and that from Africa usually shows intermediate behavior [5]. Soft cocoa butter is related to a slow crystallization rate, whilst hard butter is associated rapid crystallization [6].

As a TAG molecule can crystallize in several different crystal packing configurations, cocoa butter presents different polymorphic behaviors, on which a number of research studies have been conducted [7]. Although the type of polymorphs is a controversial subject, six different crystal polymorphisms are commonly believed to exist in cocoa butter. There are two different names to describe the polymorphs. Based on the definition by Wille and Lutton (1966) [8], the Roman numerals from I to VI are traditionally used to define cocoa butter's polymorphism in the confectionery industry, whilst  $\gamma$  (I),  $\alpha$  (II),  $\beta'$  (III),

$\beta'$  (IV),  $\beta$  (V), and  $\beta$  (VI) are frequently used to present the thermal stability and melting temperature order [7]. The relationship between those two different names has been described in De Clercq, 2011 [3]. It is reported that well-tempered chocolate is crystallized in form  $\beta$  (V), which can be obtained with a well-controlled crystallization processing via the tempering step in chocolate production [7]. However,  $\beta$  (V) form can transform into  $\beta$  (VI) form due to a long storage time and temperature fluctuations, leading to the undesirable fat bloom [9,10]. Hitherto, the amount and crystal types have been mainly measured by X-ray diffraction (XRD), differential scanning calorimetry (DSC), or pulsed nuclear magnetic resonance (pNMR) [3], while little research on the polymorphism of cocoa butter using terahertz spectroscopy has so far been carried out.

Terahertz falls in the frequency range of 0.1–10 THz (1 THz =  $10^{12}$  Hz) and the photon energy (4 meV for 1 THz) is much lower than that of X-ray photons (100 eV–100 keV) [11–13], the radiation of which is much safer for an operator in comparison of X-ray based equipment. As an emerging and cutting-edge technology, terahertz spectroscopy (THz) has been intensively employed to detect biology threats and defects [14], residue detection [15–17], transgenic food [18,19], foreign body detection [20,21], dynamical changes in seeds [22,23], and adulteration of different types of milk powder [24]. However, the application of terahertz spectroscopy in foodstuffs is still in the infant stage in comparison with the sophisticated and prevalent spectroscopic and imaging techniques like hyperspectral imaging [25–30], Raman spectroscopy [31], and NIR images [32]. This is because water is a strong THz wave absorber, which is the major hurdle for the comprehensive application of THz in the food industry [33]. With its unique transmission capability, the current application of terahertz spectroscopy to chocolate mainly focuses on detecting foreign bodies and quality (e.g., reshape due to temperature fluctuance) in packed chocolates [34–38].

Therefore, the objective of the current study is to study the feasibility of characterizing different types of crystallization from cocoa butter by using terahertz spectroscopy. This is the first study to investigate different types of crystallization from cocoa butter in the terahertz range. The feature frequency will be selected for identifying the different types of crystallization. This could potentially provide useful information for the evaluation of measurement systems, such as the measurable range and signal to noise, and the basic properties of crystallizations from different tempering procedures.

## 2. Materials and Methods

### 2.1. Sample Preparation

The sample pellets of cocoa butter (CB) were made from commercial CB purchased from a company (Ueno Ohtsuya, Tokyo, Japan). The samples were formed in a silicon cell placed on a temperature-controlled heating/cooling stage (LINKAM: 19113L). The temperature of the sample was monitored by a K-type thermocouple (TK-6200, Rixen Technology Co., New Taipei City, Taiwan).

The CB samples were first melted at 60 °C for 15 min to eliminate crystal memory and then tempered with the following procedures.

Sample A: melted CB was cooled down to −15 °C at the rate of 4.4 °C/min and stored in a freezer kept at −20 °C.

Sample B: melted CB was cooled down to 20 °C at the rate of 4.4 °C/min and kept at this temperature for 60 min. Then, the sample was slowly cooled down to 10 °C at the rate of 0.22 °C/min and stored in an incubator kept at 10 °C.

Sample C: melted CB was rapidly cooled down to 10 °C at the rate of 40 °C/min. Then, the sample was slowly frozen to −20 °C at a rate of 0.2 °C/min and stored at 4 °C.

The first two tempering processes were designed according to Marangoni and McCauley (2003) [39] and Van Malssen et al., (1999) [40].

Three types of different polymorph samples were produced in sextuplicate. After the samples were formed, the thickness was measured by a contact thickness meter (Nikon: MF-501, Tokyo, Japan) in triplicate and stored for 23 days before measurement.

## 2.2. X-ray Diffraction Measurement

The crystalline forms of the sample after 23 days of storage were measured by a  $\theta$ - $\theta$  multipurpose XRD (Rigaku, SmartLab, Tokyo, Japan) with a Cu K $\alpha$  X-ray generator ( $\lambda = 0.154056$  nm), operated at 45 kV, 200 mA. The samples were placed on a 20 mm-thick aluminum plate (Figure 1), which was precooled with ice cubes to keep the sample temperature below 10 °C during the measurement. The diffraction pattern of  $2\theta$  was corrected for 15–30° with the scanning rate of 0.05°/min. The  $2\theta$  angle was chosen according to the study of Li and Liu (2019) [41], and the data were processed by a RAS data converter. Measurement of each sample was completed within 5 min, including sample preparation and operation of XRD, to minimize crystalline change by temperature fluctuation. The temperatures inside the X-ray and the precooled aluminum plate were maintained at  $23 \pm 1$  °C and  $9 \pm 1$  °C, respectively. The original cocoa butter without any treatment was used as a control group. All samples were kept in an ice box before measurement and picked with precooled tweezers. The sample itself was held at isothermal conditions during the scans.

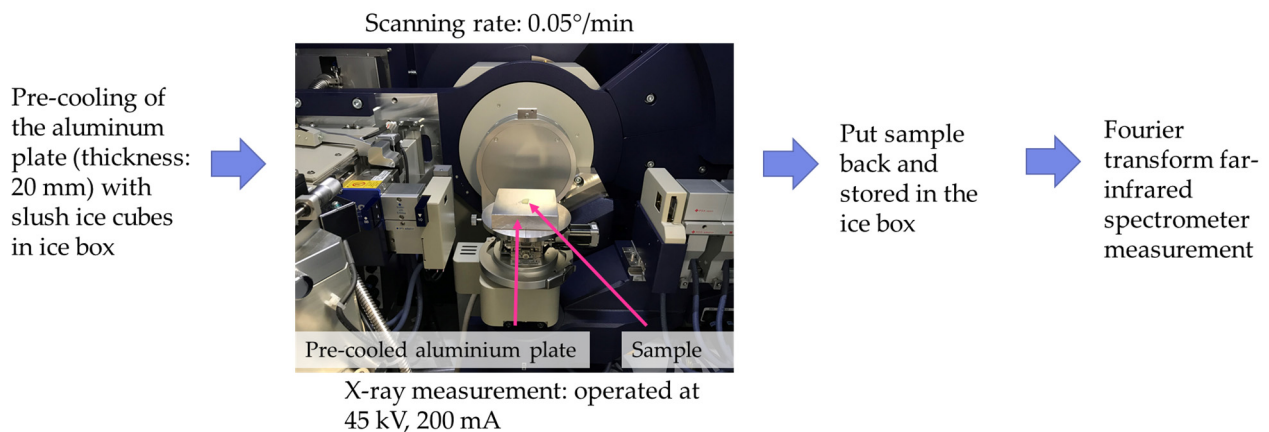


**Figure 1.** X-ray diffraction measurement experiments.

## 2.3. Terahertz Spectroscopy

THz spectra were obtained by a Fourier transform far-infrared spectrometer (FT-FIR, JASCO, FARIS, Tokyo, Japan) coupled with a superconducting bolometer (QMC Instruments Ltd., QNbB/PTC, Tokyo, Japan). A high-pressure mercury lamp was used as the light source, and a wire-grid beam splitter was used for the measurement with a resolution of 0.24 THz. A total of 200 scans were accumulated in 3 min to obtain a single spectrum.

The samples after X-ray measurement were horizontally placed on an optical aperture with a diameter of 3 mm in the sample chamber of the spectrometer. The sample chamber was purged by a continuous flow of nitrogen gas to reduce the absorption of water vapor. The nitrogen gas was cooled at  $10 \pm 1$  °C to minimize the change of the crystallinity due to the temperature rise during the measurement. The sample was left in the chamber for 5 min before measurement. In this way, the sample itself was held at isothermal conditions, and the temperature of the sample was kept constant during the scans.

The obtained spectra were converted to the absorption coefficient  $\alpha$  (cm<sup>-1</sup>) by the following equation:

$$\alpha = -\frac{1}{d} \log_{10} \left( \frac{I_s}{I_r} \right) \quad (1)$$

where  $d$  is the thickness of the sample.  $I_s$  and  $I_r$  are the power spectra of the sample and reference, respectively.

The flowchart (Figure 2) of the experiments is shown as follows:

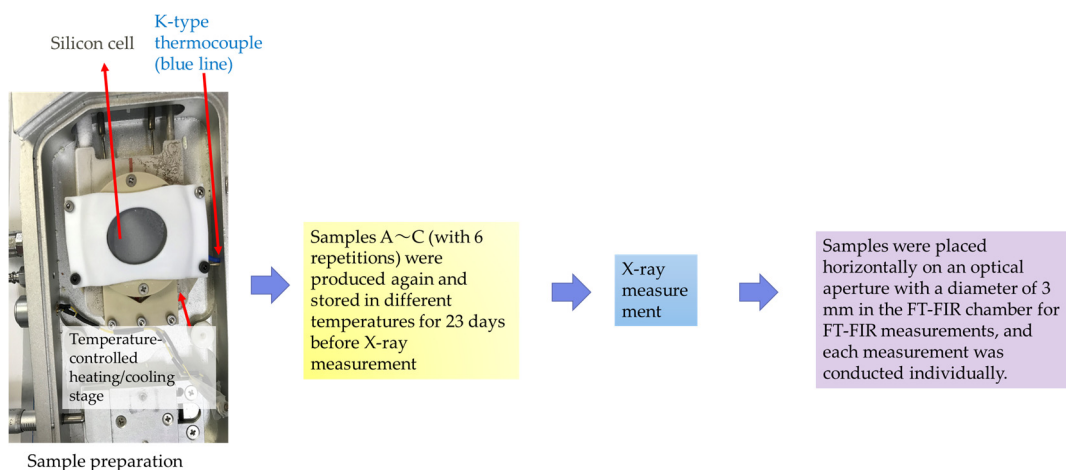


**Figure 2.** Flowchart of the experiments.

### 3. Results and Discussion

#### 3.1. Spectral Characteristics Overview for Samples Measured with XRD

Four polymorphic forms (including the original, untreated control group) of cocoa butter were determined from XRD (Figure 3). The pattern of sample A was closed to type II ( $\alpha$  type), whilst sample B and C patterns were closed to type V ( $\beta$  type) and III ( $\beta'$  type) in the studies of Wille and Lutton (1966) [8] and Talhat et al. (2015) [42], respectively. Regarding sample A, the observation of  $\alpha$  type was consistent with the study of Talhat et al. (2015), who observed the single peak at  $21.0^\circ$  in the wide-angle region (WAXS) obtained from XRD spectra [42]. Wille and Lutton (1966) stated that type II ( $\alpha$  type) products would be obtained when the melted cocoa butter was rapidly frozen and stored for several minutes to an hour at  $0^\circ\text{C}$  [8]. Marangoni and McGauley (2003) mentioned that the transient metastable  $\gamma$  and  $\alpha$  phases were generated when the temperature was below  $-15^\circ\text{C}$  [39]. However, only  $\alpha$  type was observed in the current study, which may be due to the unstable property of  $\gamma$  type as well as the longer storage time (23-d storage) before measurement [40]. The  $\alpha$  phase was reported to be much more stable than the  $\gamma$  phase and easily formed either by a transformation from the unstable  $\gamma$  or directly from the melt [8,40,42–44]. The  $\gamma$  phase was reported as the least stable of all encountered solid phases and could stay unchanged for at least 10 days only when the preset solidification temperature was lower than  $-10^\circ\text{C}$  [40]. Marangoni and McGauley (2003) claimed that the  $\gamma$  phase could be detected only after 2 days of crystallization at  $-15^\circ\text{C}$  or  $-20^\circ\text{C}$ . When the temperature increased, it transformed into  $\alpha$  type in a short time [39]. For that reason, it is difficult to define the exact melting point of the  $\gamma$  phase, and its melting or disappearing range was estimated to be around  $-8$  to  $+5^\circ\text{C}$  [40]. Van Malssen et al. (1996) mentioned that the  $\alpha$  type was generated with a cooling rate of  $360^\circ\text{C}/\text{min}$  [45]. Several authors pointed out the rapid freezing of the melted cocoa butter facilitated the  $\alpha$ -type crystallization generation [3,8,39]. However, little information on detailed processing and cooling rates was provided. This is the first study that offers specific information on how different types of crystallization are generated under different procedures with distinguished cooling rates, which could be of practical use for the chocolate industry. Although the  $\alpha$  phase is stable, it is unstable at temperatures above  $6^\circ\text{C}$  and will transfer to  $\beta'$  type (form III and IV) at most an hour [40].

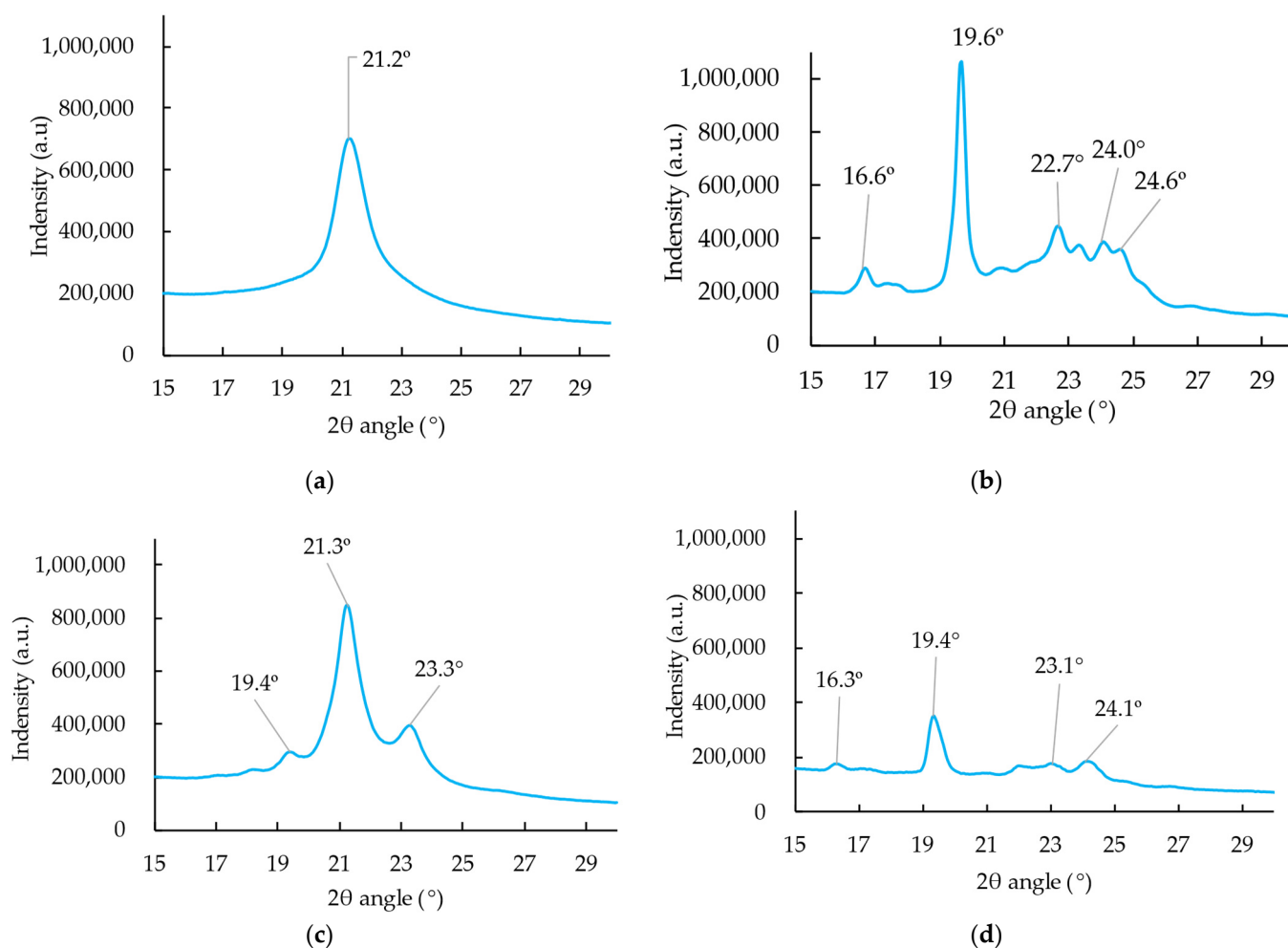


**Figure 3.** Average X-ray diffraction patterns of Sample A (a), B (b), C (c), and original untreated control sample (d).

With regard to sample B, the XRD spectra (Figure 3b) agreed with the observation from Talhat et al. (2015) [42], who found the WAXS peak at  $19.2^\circ$   $2\theta$  was more intensive and a  $1.3^\circ$  and  $2.7^\circ$  doublet formed in the range of the small angle region (SAXS) at  $27.1^\circ\text{C}$  after 2309 min [42]. Similar patterns were observed, and Sample B was defined as  $\beta$  (V) type in accordance with the study of Wille and Lutton (1966) [8]. As mentioned above, the ability to induce the formation and stabilization of certain polymorphic forms in cocoa butter is vital to producing chocolate with a fairly good quality. The presence of form V ( $\beta$  type) is in high demand as chocolate in this phase presented the desirable characteristics such as gloss, snap, and bloom resistance [4,7,9,46]. In order to maintain the quality of the chocolate, a lot of efforts have been made either to optimize the structure and presence of the  $\beta$ -type polymorph [4], to modify the crystallization of cocoa butter [47,48], or to postpone the state phase transition from  $\beta$  (V) to  $\beta$  (VI) [7,49]. All these studies accentuate an unyielding interest in obtaining  $\beta$  (V) crystal form to improve the quality of the chocolate and potentially extend the shelf life of chocolate.

According to the thermal trajectory and polymorphic forms of crystallized cocoa butter constructed by Talhat et al. (2015) [42] (Figure 4),  $\beta$  (V) type in the current study was generated in the processing of holding at  $20^\circ\text{C}$  for 60 min, which is consistent with the previous finding where  $\beta$  (V) type was formed at the temperature range of  $15\text{--}25^\circ\text{C}$  [40,42]. Numerous authors believed that  $\beta$  (V) type is transited from  $\beta'$  (type III and IV), which probably transited from the  $\alpha$  phase when the temperature increased [40,42].  $\beta$ -crystallization will be generated directly when the liquid is not memory-free, and  $\beta$ -crystallization is induced by

the memory effect [45]. However, the  $\beta$  (V) phase was always formed via the  $\beta'$  phase (type III and IV) in the study of Marangoni and McGauley (2003) [39]. The authors pointed out that  $\beta$  polymorph was obtained after 4–5 weeks at crystallization temperatures of 20 and 22 °C [39]. Although the storage temperature in the current study was set at 10 °C rather than 20 °C, the  $\beta$  polymorph generated at 20 °C during processing was stable enough to store at 10 °C.

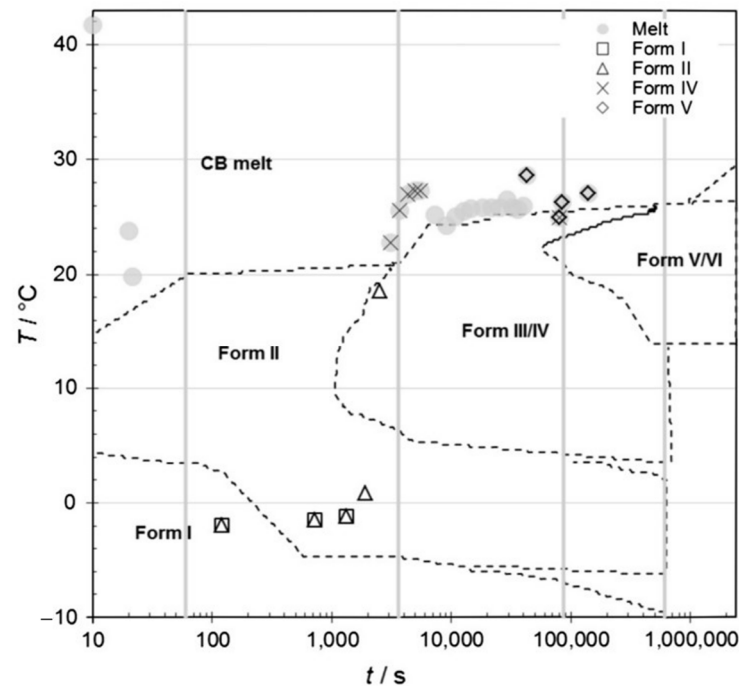


**Figure 4.** Time-temperature state diagram for the specific polymorphism of crystallized cocoa butter (cited from Talhat et al., 2015 [42]).

As for Sample C, the XRD spectra (Figure 3c) were similar to type III ( $\beta'$  type) observed by Wille and Lutten (1966) [8], who obtained type III by solidification of melt at 5 to 10 °C or by transformation of type II by storing at 5 to 10 °C. According to the procedure made for Sample C, the generated  $\beta'$  crystallization may probably follow the pathway from  $\gamma$  to  $\alpha$  and eventually reach the  $\beta'$  phase. As stated above, the rapid freezing promotes the generation of  $\alpha$  type [8], and transient metastable  $\gamma$  and  $\alpha$  phases occurred when the temperature was below  $-15$  °C. This is in agreement with the procedure for producing Sample C: rapidly cooled to 10 °C at 40 °C/min and finally froze to  $-20$  °C. Approximately 50–75% of the  $\gamma$  phase was reported to considerably transferred into the  $\alpha$  phase in at most 10 min and completed the transition in one or more days when the preset temperature was low [40]. When the temperature increases over around 5 °C, the  $\alpha$  phase is no longer stable and will transform into the  $\beta'$  formation [40], which is coincident with the procedure of Sample C, where the sample was finally stored at 4 °C.

### 3.2. Spectral Characteristics Overview for Samples after 23 Days of Storage Measured with FT-FIR

There was much noise after 8 THz, so the spectra before 8 THz were used for analysis. To clearly describe the characteristics of each sample, the average spectra were calculated by representative spectra in each group (Figure 5). The average thickness for Sample A, B, C, and the control group were  $1.72 \pm 0.05$ ,  $1.81 \pm 0.07$ ,  $1.75 \pm 0.10$ , and  $1.70 \pm 0.05$  mm, respectively. Four different patterns could be identified according to different crystallization types, which indicates that terahertz spectroscopy can, therefore, be an emerging and innovative method to control tempering in chocolate factories. There was a valley at 2.16 THz (an asterisk) for each terahertz spectrum, which may be due to the absorbance of polyethylene that was used for making the dip window. A significant change in the

THz spectral pattern of Sample B when the CB temperature was maintained at 20 °C from 30 min to 45 min. Van Malssen stated that recrystallization to the  $\beta$  (V) type that occurs within 45 min is referred to as a short-term ( $\beta$ -) memory effect, while that takes after 45 min belongs to a long-term ( $\beta$ -) memory effect [45]. Accordingly, it seems the CB may probably be a short-term ( $\beta$ -) memory effect in the current study. There was a very broad peak at 2.55 THz for Sample A ( $\alpha$  type), and the peak was shifted to 2.72 THz for Sample C [ $\beta'$  type (III)] whilst an evident sharp peak at 2.60 THz and 2.63 THz could be observed from Sample B [ $\beta$  (V) type] and control sample, respectively. No sharp peak at 1.85 THz can be obtained from Samples A, B, and C except for the original control group. Weiller et al. (2018) monitored cocoa butter in chocolate from different factories and observed peaks at 2.35 THz, 2.51 THz, 2.73 THz, and 2.97 THz from the Factory L sample, which contained one visible fat bloom [50]. For samples with 6 clear spots of fat bloom (Factory H sample), peaks at 2.41 THz and 2.65 THz can be discovered [50]. The authors claimed that the difference between the THz spectra of L and H may be due to the formation and migration of  $\beta$  (VI) associated with fatty acids [50]. The peaks at 2.55 THz from Sample A may probably be relevant to sucrose, as sucrose presents a peak at approximately 2.59 THz in the study of Nishizawa et al. (2003) [51]. According to Figure 5a,b,d, a peak at 6.80 THz can be detected from Sample A ( $\alpha$  type), B [ $\beta$  (V)], and the original control group. However, the peak at 6.80 THz for the  $\alpha$  type sample was much broader than that of the  $\beta$  type and original control type. Jiang et al. (2011) found palmitic acid possesses a distinct sharp peak at  $235\text{ cm}^{-1}$  (7.05 THz) [52], which indicates that palmitic acid—which occupies 26% of the main fatty acids of cocoa butter—may gently change in the  $\alpha$  types of crystallisations. Likewise, a comparably broad peak at 4.25 THz and 5.21 THz was observed in Sample B [ $\beta$  (V)] (Figure 5b), which may be related to the stearic acid and oleic acid that possess distinct peaks at  $154\text{ cm}^{-1}$  (4.62 THz) and  $166\text{ cm}^{-1}$  (4.98 THz), respectively [52]. In contrast, no noticeable peaks were observed from Samples A ( $\alpha$  type) and C [ $\beta'$  type (III)]. This implies that changes in stearic acid and oleic acid may occur at  $\alpha$  and  $\beta'$  type (III). The terahertz spectra shapes for  $\alpha$  and  $\beta'$  type (III) were quite similar, but the peak was shifted to the higher THz range, which may indirectly validate the pathway from  $\alpha$  to  $\beta$  type (III). Timms (2003) mentioned several different crystal packing configurations that can be formed from a TAG molecule [53]. The “three-legged” molecules can fit together in different ways, such as double-chain packing and triple-chain packing. The different polymorphs are the most apparent from a top view of the planes, which show the subcell structure [3], and in this way, three polymorphic forms, i.e.,  $\alpha$ ,  $\beta'$ , and  $\beta$  type, can be defined.

The current study is novel due to the following reasons:

1. Terahertz spectroscopy, which is much safer for operators than X-ray examination, can be a novel emerging tool to monitor cocoa butter crystallization. Previous research studies identified the types of  $\alpha$ ,  $\beta'$  (III), and  $\beta$  (V) based on XRD [8,39,40,42,43,45], the information based on identifying polymorphs cocoa butter [ $\alpha$ ,  $\beta'$  (III), and  $\beta$  (V) type] using terahertz spectroscopy has not been comprehensively exploited. This study may provide a useful fingerprint of crystallization with different phases.
2. Previous studies elaborated the general information of how each phase of crystallization formed: rapidly freezing the melted cocoa butter and storing it for several minutes to an hour at 0 °C may obtain  $\alpha$  type products [8]. The transient metastable  $\gamma$  and  $\alpha$  phases were generated if the temperature was below  $-15\text{ °C}$  [39]. This study, for the first time, provides the specific processing temperature and cooling rate that respond to each type of crystallization, which is of practical use for the tempering control for chocolate manufacturers.
3. Due to the attractive transmission capability, chocolate even packed in films or paper with high transmittance of terahertz wave, can still be utilized by using terahertz spectroscopy [50]. As stated above, the employment of terahertz spectroscopy in chocolate mostly emphasized detecting foreign bodies and quality in the packed chocolates [34–38]. It is for the first time to detect cocoa butter polymorphs of  $\alpha$ ,  $\beta'$  (III), and  $\beta$  (V) by terahertz measurement, moreover, as the XRD spectrograph

acquired in 4–5 min per sample during measurement whilst terahertz spectroscopy method needs at most 3 min per sample to identify the different polymorphs, those offer rapid detection and useful information to control cocoa butter crystallization, which is essential to chocolate factories.

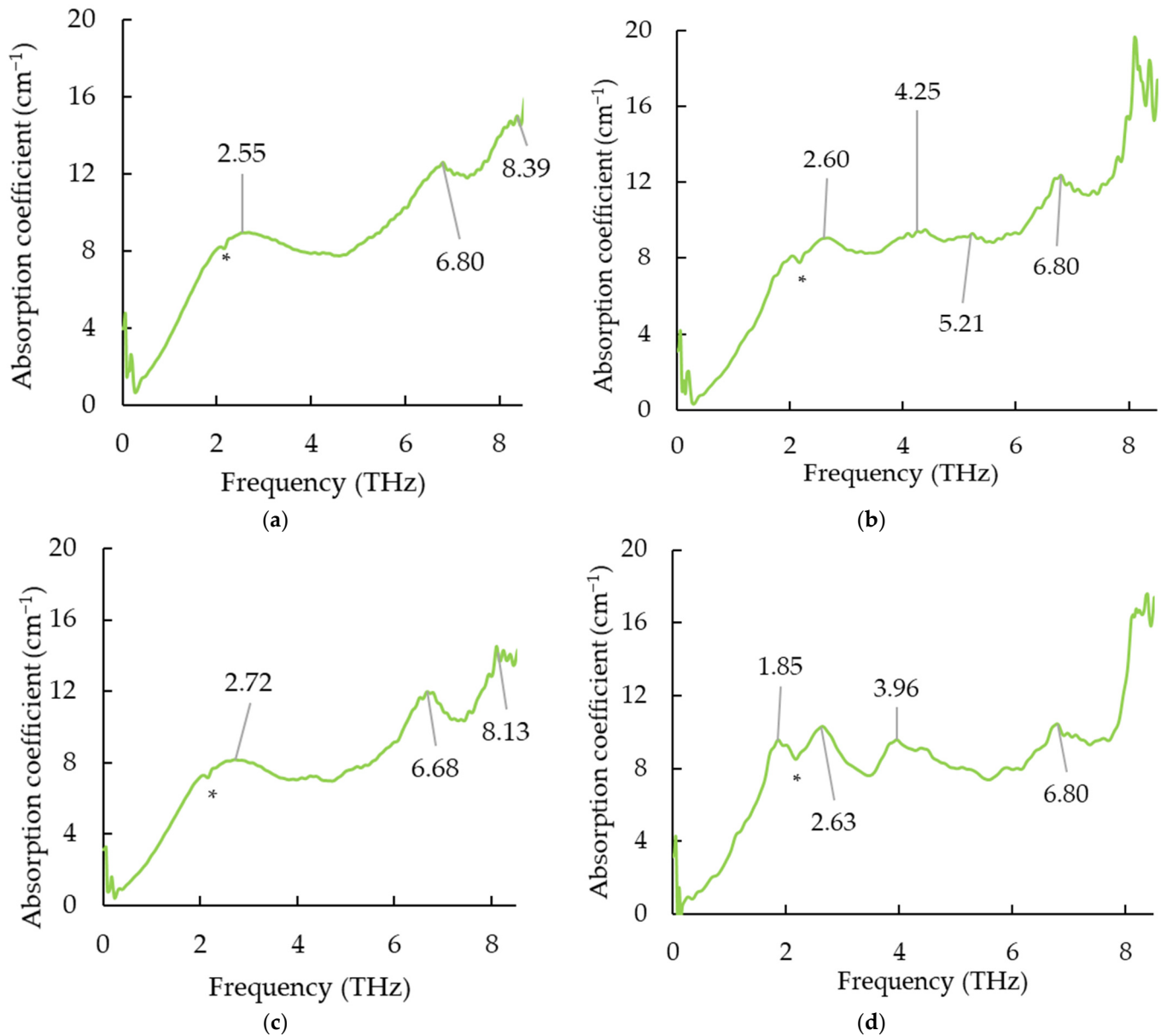


**Figure 5.** Average terahertz spectra of Sample A (a), B (b), C (c), and original untreated control sample (d). Note: There was a valley at 2.16 THz (an asterisk \*) for each terahertz spectrum, which may be due to the absorbance of polyethylene that was used for making the dip window.

#### 4. Conclusions

This research addressed characterizing different types of crystallization [i. e.,  $\alpha$ ,  $\beta'$  (III), and  $\beta$  (V) type] from cocoa butter by using terahertz spectroscopy. The specific procedures for producing  $\alpha$ ,  $\beta'$  (III), and  $\beta$  (V) types were described. Samples with different types of crystallization showed distinguished patterns of THz absorption spectra. An evident sharp peak at 6.80 THz from  $\beta$  (V) type sample and original samples was observed, whilst the  $\alpha$  type showed broad peaks. The peaks at 4.25 THz and 5.21 THz were obtained from  $\beta$  (V) type, while no noticeable peaks at those frequencies can be observed from other samples. As an emerging and promising tool to noninvasively evaluate crystallization types of cocoa

butter, the application of terahertz spectroscopy is potentially employed in the tempering control for chocolate manufacturers.

**Author Contributions:** Conceptualization, C.-H.F. and H.H.; methodology, C.-H.F. and H.H.; software, C.-H.F.; validation, C.-H.F.; formal analysis, C.-H.F. and H.H.; investigation, C.-H.F. and H.H.; resources, C.-H.F., C.O. and H.H.; data curation, C.-H.F.; writing—original draft preparation, C.-H.F., C.O. and H.H.; writing—review and editing, C.-H.F., C.O. and H.H.; visualization, C.-H.F.; supervision, C.O. and H.H.; project administration, C.-H.F. and C.O.; funding acquisition, C.-H.F. and C.O. All authors have read and agreed to the published version of the manuscript.

**Funding:** Chao-Hui Feng wishes to thank the financial support of her research work under the Special Postdoctoral Researcher Program at Riken (190021).

**Institutional Review Board Statement:** Not applicable.

**Informed Consent Statement:** Not applicable.

**Data Availability Statement:** Data are contained within this article.

**Acknowledgments:** The authors would also like to thank the anonymous reviewers for their constructive comments. Chao-Hui Feng would like to thank Yuichi Ogawa from Kyoto University for his support for her research and Yuichi Saito for the experimental setup. Chao-Hui Feng appreciates the financial support from the Leading Initiative for Excellent Young Researchers (LEADER) from the Government of Japan Ministry of Education, Culture, Sports, Science and Technology (MEXT) (2020L0277), the Japan Society for the Promotion of Science Grant-in-Aid for Early Career Scientists (20K15477), Sasakawa Scientific Research Grant from The Japan Science Society (2022–3005), FY 2022 Mishima Kaiun Memorial Foundation, Grants-in-Aid for Regional R&D Proposal-Based Program from Northern Advancement Center for Science & Technology of Hokkaido Japan (T-2-4), FY 2022 President's Discretionary Grants and FY2021 President's Discretionary Grants, funded by the Kitami Institute of Technology.

**Conflicts of Interest:** The authors declare no conflict of interest.

## References

1. Meier, B.P.; Noll, S.W.; Molokwu, O.J. The sweet life: The effect of mindful chocolate consumption on mood. *Appetite* **2017**, *108*, 21–27. [[CrossRef](#)] [[PubMed](#)]
2. Veronese, N.; Demurtas, J.; Celotto, S.; Caruso, M.G.; Maggi, S.; Bolzetta, F.; Firth, J.; Smith, L.; Schofield, P.; Koyanagi, A.; et al. Is chocolate consumption associated with health outcomes? An umbrella review of systematic reviews and meta-analyses. *Clin. Nutr.* **2019**, *38*, 1101–1108. [[CrossRef](#)] [[PubMed](#)]
3. De Clercq, N. Changing the Functionality of Cocoa Butter. Ph.D. Thesis, Ghent University, Ghent, Belgium, 2011; 220p.
4. Sonwai, S.; Podchong, P.M.; Rousseau, D. Crystallization kinetics of cocoa butter in the presence of sorbitan esters. *Food Chem.* **2017**, *214*, 497–506. [[CrossRef](#)] [[PubMed](#)]
5. Talbot, G. Vegetable fats. In *Industrial Chocolate Manufacture and Use*, 1st ed.; Beckett, S.T., Ed.; Wiley-Blackwell: West-Sussex, UK, 2009; pp. 415–433.
6. Chaiseri, S.; Dimick, P.S. Dynamic crystallization of cocoa butter. I. Characterization of simple lipids in rapid- and slow-nucleating cocoa butters and their seed crystals. *J. Am. Oil Chem. Soc.* **1995**, *72*, 1491–1496. [[CrossRef](#)]
7. Buscato, M.H.M.; Hara, L.M.; Bonomi, É.C.; Calligaris, G.D.A.; Cardoso, L.P.; Grimaldi, R.; Kieckbusch, T.G. Delaying fat bloom formation in dark chocolate by adding sorbitan monostearate or cocoa butter stearin. *Food Chem.* **2018**, *256*, 390–396. [[CrossRef](#)] [[PubMed](#)]
8. Wille, R.L.; Lutton, E.S. Polymorphism of cocoa butter. *J. Am. Oil Chem. Soc.* **1966**, *43*, 491–496. [[CrossRef](#)]
9. Rousseau, D. The microstructure of chocolate. In *Understanding and Controlling the Microstructure of Complex Foods*; McClements, D.J., Ed.; Woodhead Publishing: Cambridge, UK, 2007; pp. 648–690.
10. Talbot, G. Chocolate Temper. In *Industrial Chocolate Manufacture and Use*; Beckett, S.T., Ed.; Wiley-Blackwell: West-Sussex, UK, 2009; pp. 261–275.
11. Feng, C.-H.; Otani, C.; Ogawa, Y. Innovatively identifying naringin and hesperidin by using terahertz spectroscopy and evaluating flavonoids extracts from waste orange peels by coupling with multivariate analysis. *Food Control.* **2022**, *137*, 108897. [[CrossRef](#)]
12. Ren, A.F.; Zahid, A.; Fan, D.; Yang, X.D.; Imran, M.A. State-of-the-art in terahertz sensing for food and water security—A comprehensive review. *Trends Food Sci. Technol.* **2019**, *85*, 241–251. [[CrossRef](#)]
13. Hoshina, H.; Iwasaki, Y.; Katahira, E.; Okamoto, M.; Otani, C. Structure and dynamics of bound water in poly(ethylene-vinylalcohol) copolymers studied by terahertz spectroscopy. *Polymer* **2018**, *148*, 49–60. [[CrossRef](#)]

14. Liu, H.-B.; Zhong, H.; Karpowicz, N.; Chen, Y.Q.; Zhang, X.-C. Terahertz spectroscopy and imaging for defense and security applications. *Proc. IEEE* **2007**, *95*, 1514–1527. [[CrossRef](#)]
15. Feng, C.-H.; Otani, C. Terahertz spectroscopy technology as an innovative technique for food: Current state-of-the-Art research advances. *Crit. Rev. Food Sci. Nutr.* **2021**, *61*, 2523–2543. [[CrossRef](#)] [[PubMed](#)]
16. Qin, J.Y.; Xie, L.J.; Ying, Y.B. Rapid analysis of tetracycline hydrochloride solution by attenuated total reflection terahertz time-domain spectroscopy. *Food Chem.* **2017**, *224*, 262–269. [[CrossRef](#)] [[PubMed](#)]
17. Suzuki, T.; Ogawa, Y.; Kondo, N. Characterization of pesticide residue, cis-permethrin by terahertz spectroscopy. *Eng. Agric. Environ. Food* **2011**, *4*, 90–94. [[CrossRef](#)]
18. Liu, J.J.; Li, Z. The terahertz spectrum detection of transgenic food. *Optik* **2014**, *125*, 6867–6869. [[CrossRef](#)]
19. Liu, W.; Liu, C.H.; Hu, X.H.; Yang, J.B.; Zheng, L. Application of terahertz spectroscopy imaging for discrimination of transgenic rice seeds with chemometrics. *Food Chem.* **2016**, *210*, 415–421. [[CrossRef](#)]
20. Ok, G.; Kim, H.J.; Chun, H.S.; Choi, S.-W. Foreign-body detection in dry food using continuous sub-terahertz wave imaging. *Food Control.* **2014**, *42*, 284–289. [[CrossRef](#)]
21. Wang, C.; Zhou, R.-Y.; Huang, Y.-X.; Xie, L.J.; Ying, Y.B. Terahertz spectroscopic imaging with discriminant analysis for detecting foreign materials among sausages. *Food Control.* **2019**, *97*, 100–104. [[CrossRef](#)]
22. Li, H.; Wu, J.Z.; Liu, C.L.; Sun, X.R.; Yu, L. Study on pretreatment methods of terahertz time domain spectral image for maize seeds. *IFAC-Pap.* **2018**, *51*, 206–210.
23. Nakajima, S.; Shiraga, K.; Suzuki, T.; Kondo, N.; Ogawa, Y. Quantification of starch content in germinating mung bean seedlings by terahertz spectroscopy. *Food Chem.* **2019**, *294*, 203–208. [[CrossRef](#)]
24. Liu, J. Terahertz spectroscopy and chemometric tools for rapid identification of adulterated dairy product. *Opt. Quantum. Electron.* **2016**, *49*, 1–8. [[CrossRef](#)]
25. Rodríguez-Pulido, F.J.; Hernández-Hierro, J.M.; Nogales-Bueno, J.; Gordillo, B.; González-Miret, M.L.; Heredia, F.J. A novel method for evaluating flavanols in grape seeds by near infrared hyperspectral imaging. *Talanta* **2014**, *122*, 145–150. [[CrossRef](#)] [[PubMed](#)]
26. Rodríguez-Pulido, F.J.; Mora-Garrido, A.B.; González-Miret, M.L.; Heredia, F.J. Research progress in imaging technology for assessing quality in wine grapes and seeds. *Foods* **2022**, *11*, 254. [[CrossRef](#)] [[PubMed](#)]
27. Hu, M.-H.; Dong, Q.-L.; Liu, B.-L. Classification and characterization of blueberry mechanical damage with time evolution using reflectance, transmittance and interactance imaging spectroscopy. *Comput. Electron. Agric.* **2016**, *122*, 19–28. [[CrossRef](#)]
28. Zhuang, Q.B.; Peng, Y.K.; Yang, D.Y.; Wang, Y.L.; Zhao, R.H.; Chao, K.L.; Guo, Q.H. Detection of frozen pork freshness by fluorescence hyperspectral image. *J. Food Eng.* **2022**, *316*, 110840. [[CrossRef](#)]
29. Xie, A.G.; Sun, J.; Wang, T.M.; Liu, Y.H. Visualized detection of quality change of cooked beef with condiments by hyperspectral imaging technique. *Food Sci. Biotechnol.* **2022**, *31*, 1257–1266. [[CrossRef](#)] [[PubMed](#)]
30. Ahmed, M.; Reed, D.D.; Young, J.M.; Eshkabilov, S.; Berg, E.P.; Sun, X. Beef quality grade classification based on intramuscular fat content using hyperspectral imaging technology. *Appl. Sci.* **2021**, *11*, 4588. [[CrossRef](#)]
31. Karacaglar, N.N.Y.; Bulat, T.; Boyaci, I.H.; Topcu, A. Raman spectroscopy coupled with chemometric methods for the discrimination of foreign fats and oils in cream and yogurt. *J. Food Drug Anal.* **2019**, *27*, 101–110. [[CrossRef](#)]
32. Huang, H.; Liu, L.; Ngadi, M.O. Assessment of intramuscular fat content of pork using NIR hyperspectral images of rib end. *J. Food Eng.* **2017**, *193*, 29–41. [[CrossRef](#)]
33. Gowen, A.A.; O’ Sullivan, C.; O’ Donnell, C.P. Terahertz time domain spectroscopy and imaging: Emerging techniques for food process monitoring and quality control. *Trends Food Sci. Technol.* **2012**, *25*, 40–46. [[CrossRef](#)]
34. Koch, M. Terahertz Technology: A land to be discovered. *Opt. Photonics News* **2007**, *18*, 20–25. [[CrossRef](#)]
35. Jördens, C.; Koch, M. Detection of foreign bodies in chocolate with pulsed terahertz spectroscopy. *Opt. Eng.* **2008**, *47*, 037003. [[CrossRef](#)]
36. Schuster, F.; Coquillat, D.; Videlier, H.; Sakowicz, M.; Teppe, F.; Dussopt, L.; Giffard, B.; Skotnicki, T.; Knap, W. Broadband terahertz imaging with highly sensitive silicon CMOS detectors. *Opt. Exp.* **2011**, *19*, 7827–7832. [[CrossRef](#)] [[PubMed](#)]
37. Redo-Sanchez, A.; Laman, N.; Schulkin, B.; Tongue, T. Review of terahertz technology readiness assessment and applications. *J. Infrared Millim. Terahertz Waves.* **2013**, *34*, 500–518. [[CrossRef](#)]
38. Guillet, J.P.; Recur, B.; Frederique, L.; Bousquet, B.; Canioni, L.; Manek-Hönninger, I.; Desbarats, P.; Mounaix, P. Review of terahertz tomography techniques. *J. Infrared Millim. Terahertz Waves.* **2014**, *35*, 382–411. [[CrossRef](#)]
39. Marangoni, A.G.; McGauley, S.E. Relationship between crystallization behavior and structure in cocoa butter. *Cryst. Growth Des.* **2003**, *3*, 95–108. [[CrossRef](#)]
40. Van Malssen, K.; Van Langevelde, A.; Peschar, R.; Schenk, H. Phase behavior and extended phase scheme of static cocoa butter investigated with real-time X-ray powder diffraction. *J. Am. Oil Chem. Soc.* **1999**, *76*, 669–676. [[CrossRef](#)]
41. Li, L.L.; Liu, G.Q. Corn oil-based oleogels with different gelation mechanisms as novel cocoa butter alternatives in dark chocolate. *J. Food Eng.* **2019**, *263*, 114–122. [[CrossRef](#)]
42. Talhat, A.M.; Lister, V.Y.; Moggridge, G.D.; Rasburn, J.R.; Wilson, D.I. Development of a single droplet freezing apparatus for studying crystallisation in cocoa butter droplets. *J. Food Eng.* **2015**, *156*, 67–83. [[CrossRef](#)]
43. Van Malssen, K.F.; Peschar, R.; Schenk, H. Real-time X-ray powder diffraction investigations on cocoa butter. I. temperature dependent crystallization behavior. *J. Am. Oil Chem. Soc.* **1996**, *73*, 1209–1215. [[CrossRef](#)]

44. Jahurul, M.H.A.; Ping, L.L.; Sharifudin, M.S.; Hasmadi, M.; Mansoor, A.H.; Lee, J.S.; Noorakmar, B.W.; Amir, H.M.S.; Jinap, S.; Omar, A.K.M.; et al. Thermal properties, triglycerides and crystal morphology of bambangan (*Mangifera pajang*) kernel fat and palm stearin blends as cocoa butter alternatives. *LWT-Food Sci. Technol.* **2019**, *107*, 64–71. [[CrossRef](#)]
45. Van Malssen, K.F.; Peschar, R.; Brito, C.; Schenk, H. Real-time X-ray powder diffraction investigations on cocoa butter. III. Direct  $\beta$ -crystallization of cocoa butter: Occurrence of a memory effect. *J. Am. Oil Chem. Soc.* **1996**, *73*, 1225–1230. [[CrossRef](#)]
46. Lipp, M.; Anklam, E. Review of cocoa butter and alternative fats for use in chocolate—Part A. compositional data. *Food Chem.* **1998**, *62*, 73–97. [[CrossRef](#)]
47. Masuchi, M.H.; Grimaldi, R.; Kieckbusch, T.G. Effects of sorbitan monostearate and monooleate on the crystallization and consistency behaviors of cocoa butter. *J. Am. Oil Chem. Soc.* **2014**, *91*, 1111–1120. [[CrossRef](#)]
48. Buscato, M.H.M.; Grimaldi, R.; Kieckbusch, T.G. Cocoa butter symmetrical monounsaturated triacylglycerols: Separation by solvent fractionation and application as crystallization modifier. *J. Food Sci. Technol.* **2017**, *54*, 3260–3267. [[CrossRef](#)] [[PubMed](#)]
49. Sonwai, S.; Rousseau, D. Controlling fat bloom formation in chocolate—Impact of milk fat on microstructure and fat phase crystallisation. *Food Chem.* **2010**, *119*, 286–297. [[CrossRef](#)]
50. Weiller, S.; Tanabe, T.; Oyama, Y. Terahertz non-contact monitoring of cocoa butter in chocolate. *World J. Eng.* **2018**, *06*, 268–297. [[CrossRef](#)]
51. Nishizawa, J.; Suto, K.; Sasaki, T.; Tanabe, T.; Kimura, T. Spectral measurement of terahertz vibrations of biomolecules using a GaP terahertz-wave generator with automatic scanning control. *J. Phys. D Appl. Phys.* **2003**, *36*, 2958–2961. [[CrossRef](#)]
52. Jiang, F.L.; Ikeda, I.; Ogawa, Y.; Endo, Y. Terahertz absorption spectra of fatty acids and their analogues. *J. Oleo Sci.* **2011**, *60*, 339–343. [[CrossRef](#)]
53. Timms, R.E. *Confectionery Fat Handbook*; The Oily Press: Bridgwater, UK, 2003.

**Disclaimer/Publisher’s Note:** The statements, opinions and data contained in all publications are solely those of the individual author(s) and contributor(s) and not of MDPI and/or the editor(s). MDPI and/or the editor(s) disclaim responsibility for any injury to people or property resulting from any ideas, methods, instructions or products referred to in the content.